Modeling of Calcium Oxalate and Amorphous Silica Composite Fouling

Hong Yu and Roya Sheikholeslami
School of Chemical Engineering and Industrial Chemistry, The University of New South Wales, Sydney, New South Wales, Australia

William O. S. Doherty
Sugar Research Institute, Mackay, Queensland, Australia

DOI 10.1002/aic.10397
Published online February 28, 2005 in Wiley InterScience (www.interscience.wiley.com).

An analytical model has been used to describe the composite scale formation of calcium oxalate monohydrate (COM) and amorphous silica (SiO_2) in sugar solutions. The model incorporated the effects of the liquid bulk subcooling and deposition consolidation process arising from microlayer evaporation under subcooled nucleate flow boiling. The proposed model was shown to provide a better fit to the COM–SiO_2 composite fouling data than models considering only particulate fouling or silica deposition over a range of process thermal hydraulic parameters which included surface temperature, fluid velocity and bulk subcooling. For a better description of the composite fouling process in sugar factory, it is suggested that the effects of solution pH and composition on composite fouling be considered in future work. © 2005 American Institute of Chemical Engineers *AIChE J,* 51: 1214–1220, 2005

Keywords: composite fouling, calcium oxalate, amorphous silica, sugar mill evaporator, modeling

Introduction

The deposition of nonsugar scales is known to cause serious processing problems in sugar mills by reducing the thermal hydraulic performance of the multieffect evaporator station, which accounts for about 70% of the total energy consumption of a sugar mill.[1-3] Composite deposits containing calcium oxalate (CaOx) and SiO_2 are particularly problematic because of their tenacious nature for conventional cleaning techniques, which are either inefficient or costly. Special chelating reagents such as EDTA are necessary to effectively remove these deposits from the evaporator.[1] Thus there is a growing interest in the development of more cost-effective scale control and removal strategies to minimize the composite fouling of CaOx–SiO_2 in sugar mill evaporators.

The composite fouling of CaOx [as calcium oxalate monohydrate (COM), the most stable hydrate form of CaOx under high temperatures] and SiO_2 in water and sugar solutions has been the subject of a systematic investigation by the authors with the latest work relating the effects of various operating conditions to the mechanisms of composite fouling.[4-6] The results indicated that the primary mechanism of composite fouling was particulate deposition of COM–SiO_2 colloidal species. The active interfacial forces involved were believed to be attractive van de Waals forces and the repulsive electrical double-layer forces. The rate of composite fouling was found to increase with decreasing interfacial energy barrier between the surface of heat exchange tube and the COM–SiO_2 colloidal particle as a result of the interactions of these forces. Thus composite fouling was likely to be a surface-controlled process.[6]

In addition to the role of interfacial forces in controlling

Correspondence concerning this article should be addressed to R. Sheikholeslami at this current address: Dept. of Chemical and Biological Engineering, University of British Columbia, 2216 Main Mall, Vancouver, BC V6T 1Z4, Canada; e-mail: r.sheikholeslami@chml.ubc.ca.

particle deposition rate, the rate of composite fouling and the characteristics of the deposits were also found to be strongly dependent on the surface superheat, fluid velocity, and bulk subcooling.[5] First, the composite fouling rate increased with increasing superheat as a result of enhanced bubble–particle interactions at the boiling surface. For a constant superheat, the fouling rate reached a maximum at an intermediate subcooling but remained relatively constant over a range of fluid velocity. Second, the composite deposit was found to exhibit higher bonding strength than silica scales as a result of structural consolidation by COM in the silica matrix under subcooled nucleate boiling. The consolidation process led to a linear, rather than asymptotic, fouling rate for composite fouling. The extent of deposit consolidation was shown to increase with superheat, fluid velocity, and subcooling.[5]

To evaluate and obtain strategies to effectively mitigate the composite fouling of COM and SiO_2, it is essential to be able to make predications of the rate of composite fouling. This will also facilitate the development of improved design and operation of the evaporator station. This paper, therefore, presents the results on the modeling of the COM–SiO_2 composite fouling based on the effects of various thermal hydraulic operating parameters and some of the previously proposed mechanistic assumptions.[5] In particular, deposit consolidation by COM in the matrix of SiO_2 is considered through microlayer evaporation. The model predictions are compared with experimental data for a constant solution pH and composition (that is, initial COM and SiO_2 supersaturations and sugar concentration). Factors that influence key concepts and parameters of the composite fouling model are briefly discussed.

Experimental

Details of the experimental setup and test conditions used in this work have been provided elsewhere.[4] In brief, the closed-loop circulation system includes a circulation pump; a storage tank; an annular test section (Pegasus, Canada); a cooling heat exchanger; a level control system (Burkert Contromatic Australia P/L); series of pressure, temperature, and flow measuring and control devices; and a PC with a data acquisition and control system (DA&C, Genie, American Advantech Co.). The experiments were conducted under constant solution composition and subcooled flow boiling with major operating parameters such as surface superheat, fluid velocity, and bulk subcooling maintained in ranges comparable to those usually encountered in the later effects of a sugar mill evaporator. A constant sugar concentration of 25% (w/w) was used. This is typical of the juice concentration exiting the second effect of a quintuple evaporator set in a sugar mill.

Synthetic juice solutions were prepared from a commercial sugar (purity 99.5%), kindly supplied by Sugar Australia, Pty, Ltd., NSW. HCl and NaOH were used to adjust the initial pH of the tank solutions to 6.5. All the other chemicals used were analytical-grade reagents. Data collection was initiated after all the chemicals were mixed in the tank. The changes in the concentrations of COM and SiO_2 (both reactive and colloidal forms of silica) were monitored through periodic sample withdrawal. Calcium, oxalate, and both total and reactive SiO_2 contents in the withdrawn samples were determined using ICP-AES (inductively coupled plasma–atomic emission spectrometer; Varian Vista AX) and UV-visible spectroscopy (Varian Cary 1E spectrophotometer). After dynamic experiments, the resulting scales were characterized by SEM-EDS (Hitachi S4500). The zeta-potential values of scale particles were determined from electrophoretic mobility measurements (Brookhaven PALS zeta-potential analyzer). The bulk densities of scales were estimated by weighing the different samples and measuring their volumes. The thermal conductivity of scales was estimated from the calculated fouling resistance and measurements of deposit layer thickness.

Results and Discussion

Previous modeling works

Most mathematical models of particulate fouling available in the literature are based on a general material balance equation proposed by Kern and Seaton[7]

$$\frac{dm_t}{dt} = \phi_d - \phi_r \tag{1}$$

where m_t is the amount of deposit after time t, ϕ_d is the deposition rate, and ϕ_r is the removal rate. Considering a constant deposition rate and an increasing removal rate with the mass of deposit, the integrated form of Eq. 1 in terms of fouling resistance may be expressed by

$$R_f = R_f^*(1 - e^{-Bt}) \tag{2}$$

where $R_f^*(=\phi_d/B)$ is the asymptotic fouling resistance and B is a constant related to deposit strength. The deposition rate was proposed to be a function of bulk concentration of fouling species (C_b) and fluid velocity (υ), whereas the removal rate was dependent on wall shear stress (τ) and deposit thickness (x_f)

$$\phi_d = K_1 C_b \upsilon \tag{3}$$

$$\phi_r = K_2 \tau x_f = K_3 \upsilon^2 R_f \tag{4}$$

where K_1, K_2, and K_3 are constants. The basic concept of the Kern–Seaton model (Eq. 1) has been widely used for the development of fouling models, such as the Watkinson–Epstein model, the Gudmundsson model, the Epstein model, and the Melo–Pinheiro model, which have different functional expressions of ϕ_d and ϕ_r (see Table 1), depending on the specific fouling species and mechanisms involved. Features of these models have been reviewed by Epstein[8,9] and Pinheiro.[10]

Turner and Klimas[15] proposed a particulate fouling model to include the effect of deposit consolidation on the kinetics of fouling under flow boiling conditions

$$\frac{dm_t}{dt} = K_d C - K_r m_r(t) \tag{13}$$

$$\frac{dm_r}{dt} = \frac{dm_t}{dt} - K_c m_r(t) \tag{14}$$

where m_t is the total deposit mass, m_r is the part of the total deposit mass available to be removed, and C is the concentra-

Table 1. Summary of Fouling Models Derived from Kern–Seaton Concept

Model	Deposition Term	Removal Term	Applicable Conditions
Watkinson and Epstein[11]	$\phi_d = NP = K_d(C_b - C_s)P$ (5) $P = \frac{K_4 e^{-(E/RT_s)}}{v^2 f}$ (6)	Same as the Kern–Seaton model (Eq. 4)	Particulate fouling
Gudmudsson[12]	Same as above	$\phi_r = K_5 v R_f$ (7)	Particulate fouling; also correlates gas–oil fouling data
Taborek et al.[13]	$\phi_d = K_6 P_d \Omega^n e^{-(E/RT_s)}$ (8)	$\phi_r = K_7 \frac{\tau}{\psi} x_f$ (9)	$CaCO_3$ crystallization fouling in the presence of particulate matters
Melo and Pinheiro[14]	$\phi_d = \frac{C}{1/K_t + 1/K_r}$ (10)	$\phi_r = K_8 v^{2-a} R_f$ (11)*	Generalized model
Epstein[8]	$\phi_d = \frac{C}{\frac{k' \mathrm{Sc}^{2/3}}{v^*} + \left[\frac{k'' e^{E/RT_s}(v^*)^2}{v \phi_d^{n-1}}\right]^{1/n}}$ (12)	n/a	Initial chemical reaction and particulate fouling, verified for colloidal particles and surface charge effects

*$a \approx 1$ for kaolin–water systems at high Reynolds numbers (7000–12,000), where surface adhesion controlled the deposition process.

tion of particles in solution. K_r and K_c are the removal and consolidation rate coefficients, respectively. Equations 13 and 14 could be combined and integrated to the following expression of m_t

$$m_t = \frac{K_d C}{K_r + K_c}\left\{tK_c + \frac{K_r}{(K_r + K_c)^2}\left(1 - e^{[-(K_r + K_c)t]}\right)\right\} \quad (15)$$

Thus the model assumed the existence of a deposit bilayer consisting of a consolidated inner layer surrounded by an unconsolidated loose layer, and was capable of predicting different fouling kinetic profiles, depending on the relative magnitudes of K_d, K_r, and K_c. For high rates of deposit consolidation, the above equation simplified into a linear kinetics form

$$m_t = K_d C \frac{K_c}{K_r + K_c} t \quad (16)$$

Turner and Klimas proposed that deposit consolidation be considered a process in which a chemical bond was formed between the particle and the heat transfer surface or predeposited film. Potential mechanisms for deposit consolidation included Ostwald ripening, dissolution–recrystallization, and boiling-induced precipitation of the dissolved species in the pores of the deposit. Therefore, the rate of consolidation, especially under boiling conditions, was strongly affected by factors such as heat flux.

The effect of heat flux on the deposition of iron oxide particles on boiling surface was previously demonstrated by Asakura et al.,[16] who formulated a model based on microlayer evaporation

$$\frac{dm_t}{dt} = \frac{Kq''C}{h_{fg}} \quad (17)$$

where q'' is heat flux, h_{fg} is the latent heat, C is the particle concentration in solution, and $q''C/h_{fg}$ is the amount of particles contained in the vaporized water during nucleate boiling. K is the deposition rate coefficient representing the fraction of particles that deposited on the surface

$$K = \left(\frac{4}{3}\right)^2 R_b U \frac{\rho_G^2}{\rho_l} \nu_l \quad (18)$$

where R_b is the maximum bubble radius and U is the bubble growth rate.

Chan et al.[17] derived a model that could predict the deposition of silica from geothermal brines in tubular heat exchangers as a function of silica supersaturation and pH

$$\frac{dR_f}{dt} = K_R\left(\frac{C_b - C_e}{C_e}\right)^p (C_{\mathrm{OH}^-})^r \quad (19)$$

where K_R is the deposition rate constant, C_b is the bulk concentration of silica, C_e is the silica solubility at surface temperature, C_{OH^-} is the molar concentration of OH^- ions in the bulk solution, and p is the reaction order of silica. The thermal hydraulic conditions were accounted for in the model by evaluating their effects on surface temperature.

Composite fouling model

The model used for the present study was developed based on the concept of the Turner–Klimas model[15] (Eq. 16), given that deposit consolidation has been found to be a significant mechanism affecting the rate of composite fouling and the structure of the deposits

$$R_f = \frac{K_d C_{\mathrm{SiOH_2}}}{\rho_f k_f} \frac{\phi_c}{\phi_r + \phi_c} t \quad (20)$$

where ρ_f and k_f are density and thermal conductivity of the deposit, respectively. $C_{\mathrm{SiO_2}}$ is the concentration of colloidal silica, which is the major source of particles in solution. The

Table 2. Parameter Values of Composite Fouling Model for CaOx–SiO_2 Binary Systems in Sugar Solutions

Run	Superheat (K)	Heat Flux (kW/m^2)	Velocity (m/s)	Subcooling (K)	A ($\times 10^{-5}$)	K' ($\times 10^{-17}$)	A/K' ($\times 10^{11}$)
1	5	56.4	1.1	20	3.4	9.9	3.4
2	10	67.9	1.1	20	5.9	13.0	4.5
3	15	80.4	1.1	20	12.8	14.3	9.0
4	10	48.0	0.8	20	3.3	200.0	1.7
5	10	79.4	1.4	20	2.2	3.6	6.1
6	10	79.4	1.1	25	10.0	14.0	7.1
7	10	87.7	1.1	30	120	200.0	6.0
8	10	104.9	1.8	20	1.9	1.7	11.2

determination of deposition, removal, and consolidation terms (that is, K_d, ϕ_r, and ϕ_c) are described below.

(1) Deposition. The Watkinson–Epstein model and the Pinheiro model were used to formulate the deposition term. Under the operating conditions used in this work, deposition was a surface-controlled process, which can be expressed in a modified deposition term of the Watkinson–Epstein model for adhesion control by assuming that the interfacial energy barrier for particle attachment was applicable to boiling conditions

$$K_d = \frac{Ae^{-(E/RT_s)}}{v^2} \tag{21}$$

where A is a preexponential factor that includes the effects of all the other variables apart from T_s.[10] K_d was considered to have a strong velocity dependency similar to that demonstrated for the deposition of kaolin and silica under turbulant flow conditions.[14,18]

(2) Removal. The removal term was derived based on the Pineiro model as follows

$$\phi_r = K' v^{2+b} \tag{22}$$

where b is a constant representing the effect of enhanced hydrodynamic lift forces arising from changes in fluid viscosity (subcooling effect).[5] K' is a coefficient with a physical meaning similar to that of A (that is, representing effects other than those of velocity and subcooling[10]). If a linear relationship was assumed between the removal rate and fluid viscosity,[19] the above equation becomes

$$\phi_r = K' v^3 \tag{23}$$

(3) Consolidation. The Asakura et al. model was used to define the rate of consolidation during composite fouling by considering COM precipitation through microlayer evaporation only under constant heat flux operation mode,[5] that is

$$\phi_c = \frac{C_{\mathrm{COM}} q''}{h_{fg} + c_p \Delta T_{sub}} K_c \tag{24}$$

where C_{COM} is the concentration of COM in solution, c_p is the fluid specific heat, ΔT_{sub} is the bulk subcooling, and K_c has the same expression as Eq. 18. The values of R_b and U in Eq. 18 were obtained from published data.[16] The composite fouling resistance in terms of thermal hydraulic operating conditions was obtained by combining Eqs. 20–24; thus

$$R_f = \frac{A \exp(-E/RT_s) C_{\mathrm{SiO_2}}}{v^2 k_f \rho_f (K'M + 1)} t \tag{25}$$

$$M = \frac{v^3 (h_{fg} + c_p \Delta T_{sub})}{K_c q'' C_{\mathrm{COM}}} \tag{26}$$

With the above two equations and Eq. 18 it is possible to determine the composite fouling rates as a function of heat flux, fluid velocity, and bulk subcooling. Other necessary input parameters include concentrations of COM and SiO_2 and thermophysical properties of liquid and steam (which can be determined directly based on surface or bulk temperature). Only A and K' have to be determined through individual data-set fitting (that is, Eq. 25).

Comparison of models with composite fouling data

The Chan et al. silica deposition model, the Watkinson–Epstein particulate fouling model, and the composite fouling model proposed in the present study have been compared with the available composite fouling data. The fitted values of A and K' for the composite fouling model are summarized in Table 2. It is apparent that the ratio between A and K' linearly increased from 1.7×10^{11} at heat flux 48 kW/m^2 to 11.2×10^{11} at heat flux 105 kW/m^2 (Figure 1), reflecting a higher degree of deposit consolidation at a higher heat flux level. A somewhat similar trend was observed for K_R values in the Chan et al. model (Figure 2), except that the latter gave more scatter

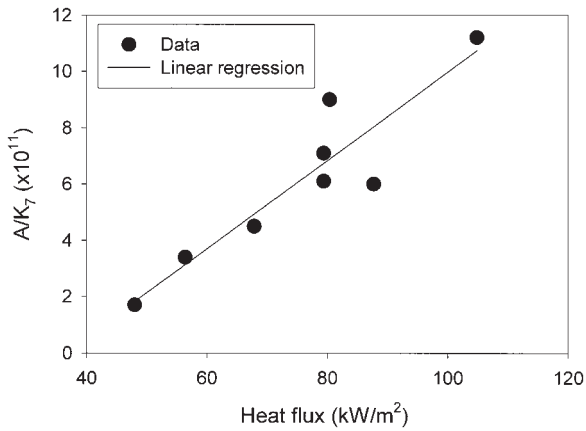

Figure 1. Changes in the calculated parameters for the composite fouling model as a function of heat flux.

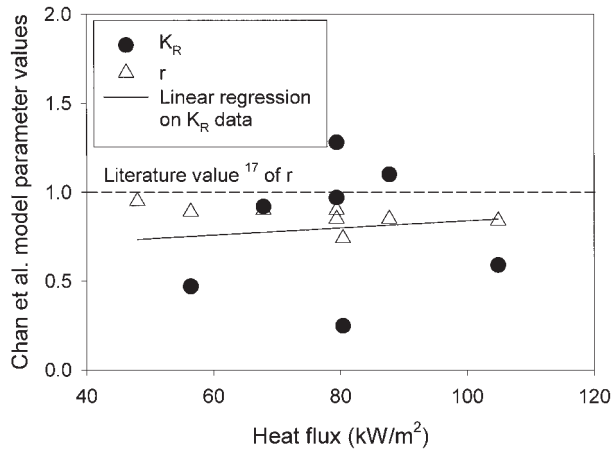

Figure 2. Chan et al. model parameters in comparison to literature value.

K_R data for Run 4 not included.

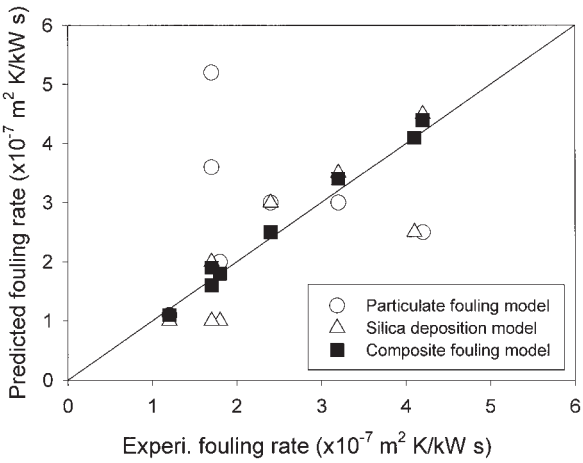

Figure 4. Comparison of experimental data with model predictions.

around linearity, presumably because the effects of thermal hydraulic parameters other than heat flux were not considered in this model. The value of r in the Chan et al. model was found to vary in the range of 0.8–0.95, which was in reasonable agreement with the published data of 1.0.[17] The parameter values of K_d/K_3 in the Watkinson–Epstein model are shown in Figure 3. In contrast to the trend given by the composite fouling model, the linear regression on these data indicated a reduced K_d/K_3 with increasing heat flux.

Figure 4 shows that experimental data were better predicted by the proposed composite fouling model for all conditions with a mean deviation of less than 6%, which was of similar magnitude to the experimental error.[4] The mean deviations of data fits for the Watkinson–Epstein model and the Chan et al. silica deposition model ranged from 25 to 35%. Other particulate fouling models from the literature have also been tested with results similar to those of the above two models (deviations of about 30–35% for the Epstein model and the Taborek et al. model). The differences in the model fits demonstrated the advantages of composite fouling model in describing CaOx–SiO_2 composite fouling behavior by accounting for the interactive effects between CaOx and SiO_2 under subcooled boiling, which resulted in deposit consolidation, and the bulk subcooling effect. Therefore, the poor data fits by the other models were not surprising, given that they were not derived to specifically involve these effects, which were critical to the reliable analysis of composite fouling process.

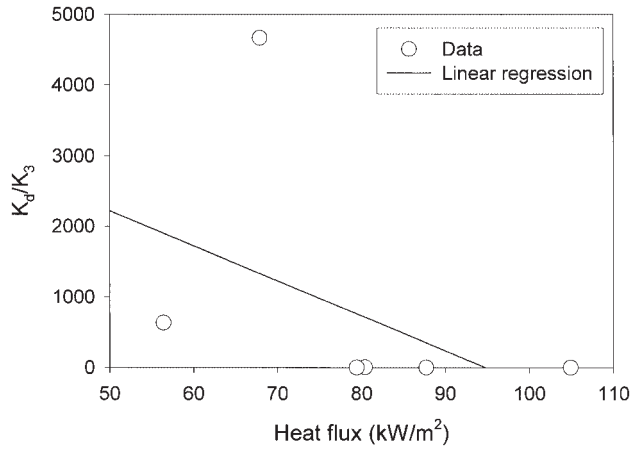

Figure 3. Watkinson and Epstein model parameters.

Data for Run 4 not available.

A major feature of the model presented in this article, in contrast to previous particulate fouling models, was that the effects of thermal hydraulic parameters on the rate of deposit consolidation during the fouling process were considered to be based on the mechanism of microlayer evaporation, which was directly proportional to the heat flux as was demonstrated in the Asakura et al. model (Eq. 17). Because the heat flux increased with increasing fluid velocity and bulk subcooling, the higher velocity and subcooling also indirectly contributed to a higher degree of microlayer evaporation, and thus deposit consolidation.[5]

Liquid bulk subcooling was one of the key elements in composite fouling model proposed by the authors. Apart from the role of changing the rate of deposit consolidation, there are other ways in which subcooling could affect the model parameters. First, the physical properties of solution, such as viscosity, are dependent on bulk temperature. Higher solution viscosity with increasing subcooling could affect the hydrodynamic lift forces at the wall and the removal rate of the deposit. Second, colloidal COM–SiO_2–sugar complexes acquired their surface charges through the dissociation of a proton from the hydroxyl groups, that is

$$-\mathrm{SOH} \overset{K_a}{\Longleftrightarrow} -\mathrm{SO}^- + \mathrm{H}^+ \tag{27}$$

$$-\mathrm{SOH}_2^+ \overset{K_b}{\Longleftrightarrow} -\mathrm{SOH} + \mathrm{H}^+ \tag{28}$$

where K_a and K_b are the dissociation constants of Eqs. 27 and 28, respectively. The charge or the degree of dissociation of these species was governed by the dissociation constants, which are always dependent on pH and temperature. An increase in the point of zero charge (pzc) [pzc = $(pK_a + pK_b)/2$] of colloidal species could be obtained by decreasing the bulk

Table 3. Surface Zeta-Potential of Sample Particles Obtained at Different Subcooling Levels

Bulk Subcooling (K)	Surface Zeta-Potential of Particle (mV)
20	−26.3*
25	−25.7
30	−24.9

*Average of six runs.

temperature if the above equilibria were endothermic,[20] given that fewer hydroxyl groups became negatively charged as a result of proton release. While the surface charge of the heat exchange tube remained unchanged for a constant surface temperature, a reduction in the surface charge of the particle would affect the particle attachment efficiency by reducing the energy barrier at the particle–heat exchange tube interface. The former (viscosity) effect has been accounted for by the use of higher velocity dependency of removal rate based on previous work by Williams et al.,[19] whereas the latter (surface charge effect) was not included in the model because it was unlikely that this constituted any significant contribution toward the model parameters, given the limited range of bulk subcooling values used in the present study (see Table 3). It should be noted, however, that the actual surface charge variation in a sugar factory could be much more complex than that portrayed here because of the variations in solution pH and the concentrations of sugar, CaOx, and SiO_2, which might also have a significant impact on the deposit removal and consolidation processes. Although this is beyond the scope of the present study, further work to verify and incorporate these effects into the existing or other new mechanistic model are recommended to provide a better prediction of the composite fouling process in sugar mill evaporators.

Conclusions

A composite fouling model, which took into account the additional effects of deposit consolidation and bulk subcooling, has been developed in this work to describe the COM–SiO_2 composite fouling in an evaporator unit. The rate of fouling could be better predicted by the proposed model, compared to other fouling models, over a range of thermal hydraulic parameters under a subcooled flow boiling condition. However, the effects of solution pH and composition on the overall composite fouling process could not be determined from the model and further experiments and model refinement would be required in the future to establish the contribution of these parameters.

Acknowledgments

This work was supported by an Australian Research Council Linkage Project Grant (previously the ARC-SPIRT Scheme). We thank Sugar Australia P/L, NSW, especially P. Hayes, for providing sugar and its delivery arrangement. The financial support of the Sugar Research Institute (SRI) of Australia is gratefully acknowledged.

Notation

A = preexponential constant in Eq. 21
a = empirical parameter in Eq. 11
b = constant in Eq. 22
B = parameter related to deposit strength in Eq. 2, s^{-1}
c_p = heat capacity, J kg^{-1} $°C^{-1}$
C = concentration of particles, kg/m^3
C_e = equilibrium concentration at surface temperature (Eq. 18)
C_{OH^-} = molar concentration of OH^- ions
D_m = molecular diffusivity, m^2/s
E = activation energy, kJ g^{-1} mol^{-1}
f = Fanning friction factor
h_{fg} = latent heat of vaporization, J/kg
k = thermal conductivity, W m^{-1} K^{-1}
k' = mass transfer constant in the Epstein model (Eq. 12)
k'' = attachment constant in the Epstein model (Eq. 12)
K = deposition rate coefficient in the Asakura model (Eq. 16), m/s
K_{1-3} = constants in the Kern and Seaton model (Eqs. 3 and 4)
K_4 = constant in the Watkinson and Epstein model (Eq. 6)
K_5 = constant in the Gudmundsson model (Eq. 7)
K_6 = constant in the Taborek et al. model (Eq. 8)
K_7 = constant in the Taborek et al. model (Eq. 9)
K_8 = constant in the Melo and Pinheiro model (Eq. 11)
K' = constant in the composite fouling model (Eq. 21)
$K_{a,b}$ = surface dissociation constants, L/mol
K_c = consolidation rate coefficient, m/s
K_d = deposition rate coefficient, m/s
K_r = removal rate coefficient, m/s
K_R = deposition rate coefficient in the Chen et al. model (Eq. 18), m/s
K_t = transport rate coefficient in the Melo and Pinheiro model (Eq. 10), m/s
m = amount of deposit, kg/m^2
n = constants in the Taborek et al. model (Eq. 8) and the Epstein model (Eq. 12)
N = mass flux normal to the wall, kg m^{-2} s^{-1}
P = sticking probability in Eq. 5
P_d = probability function in Eq. 8
p = reaction order
q'' = heat flux, kW/m^2
r = constant in Eq. 15
R = universal gas constant, J K^{-1} mol^{-1}
R_b = maximum bubble radius, m
R_f = fouling resistance, m^2 K^{-1} kW^{-1}
R_f^* = asymptotic fouling resistance, m^2 K^{-1} kW^{-1}
Sc = Schmidt number ($= \nu/D_m$)
t = time, s
T = temperature, K
ΔT_{sub} = subcooling, K
U = bubble growth rate, m/s
x_f = deposit thickness, m

Greek letters

ϕ_c = consolidation rate, kg m^{-2} s^{-1}
ϕ_d = deposition rate, kg m^{-2} s^{-1}
ϕ_r = removal rate, kg m^{-2} s^{-1}
ρ = density, kg/m^3
ν = kinematic viscosity (μ/ρ), m^2/s
ψ = deposit strength factor in the Taborek et al. model (Eq. 9)
τ = shear stress, N/m^2
υ = fluid velocity, m/s
υ^* = friction velocity ($= \upsilon\sqrt{f/2}$), m/s
Ω = water characterization factor in the Taborek et al. model (Eq. 8)

Subscripts

b = bulk
COM = calcium oxalate monohydrate
f = foulant
G = gas
l = liquid
r = removable
s = surface
SiO_2 = silica

Literature Cited

1. Doherty WOS. Chemical cleaning of sugar mill evaporator. *Proc Aust Soc Sugar Cane Technol.* 2000;22:341-346.
2. Walthew DC. Aspects of evaporator scale formation and control in the

South African sugar industry. Proc. of Conf. on Sugar Processing Research; 1996:22-43.
3. Walthew DC, Khan F, Whitelaw R. Some factors affecting the concentration of silica in cane juice evaporators. *Proc South African Sugar Technol Assoc*. 1998;72:223-227.
4. Yu H, Sheikholeslami R, Doherty WOS. Composite fouling characteristics of calcium oxalate monohydrate and amorphous silica by a novel approach simulating successive effects of sugar mill evaporator. *Ind Eng Chem Res*. 2002;41:3379-3388.
5. Yu H, Sheikholeslami R, Doherty WOS. Effects of thermal-hydraulic conditions on fouling of calcium oxalate and silica. *AIChE J*. 2005; 51(2):641-648.
6. Yu H, Sheikholeslami R, Doherty WOS. Deposition of composite scale of calcium oxalate and silica from synthetic juice solutions, Proc. of CHEMECA '03, paper 118 (CD-ROM), Adelaide, Australia, October; 2003.
7. Kern DQ, Seaton RE. Theoretical analysis of thermal surface fouling. *Br Chem Eng*. 1959;4:258-262.
8. Epstein N. Elements of particle deposition onto nonporous solid surfaces parallel to suspension flows. *Exp Therm Fluid Sci*. 1997;14:323-334.
9. Epstein N. Particle deposition and its mitigation, Proc. of Int. Conf. on Understanding Heat Exchanger Fouling and Its Mitigation, Castelvecchio Pascoli, Italy; 1999.
10. Pinheiro JRS. Fouling of heat transfer surfaces. In: Palen JW, ed. *Heat Exchanger Sourcebook*. Washington, DC: Hemisphere Publishing; 1986:721-743.
11. Watkinson AP, Epstein N. Particulate fouling of sensible heat exchangers, Proc. 4th Int. Heat Transfer Conf., Versailles, France; 1970.
12. Gudmundsson JS. *Fouling of Surfaces*. PhD Thesis. Birmingham, UK: University of Birmingham; 1979.
13. Taborek J, Aoki T, Ritter RB, Palen JW. Predictive methods for fouling behaviour. *Chem Eng Prog.* 1972;68:69-78.
14. Melo LF, Pinheiro JD. Particulate fouling: Controlling processes and deposit structure, Proc. 8th Int. Heat Transfer Conf., San Francisco, CA, Aug. 17–22; 1986.
15. Turner CW, Klimas SJ. The effect of surface chemistry on particulate fouling under flow-boiling conditions, Proc. 4th Int. Conf. on Heat Exchanger Fouling, Fundamental Approach and Technical Solutions, Davos, Switzerland; 2001.
16. Asakura Y, Kikuchi M, Uchida S, Yusa H. Deposition of iron oxide on heated surfaces in boiling water. *Nucl Sci Eng*. 1978;67:1-7.
17. Chan SH, Rau H, Debellis C, Neusen KF. Silica fouling of heat transfer equipment—Experiments and model. *J Heat Transfer*. 1988; 110:841-49.
18. Yiantsios SG, Karabelas AJ. Deposition of micron-sized particles on flat surfaces: Effects of hydrodynamic and physicochemical conditions on particle attachment efficiency. *Chem Eng Sci.* 2003;58:3105-3113.
19. Williams PS, Moon MH, Xu YH, Giddings JC. Effect of viscosity on retention time and hydrodynamic lift forces in sedimentation/steric field-flow fractionation. *Chem Eng Sci.* 1996;51:4477-4488.
20. Akratopulu KC, Kordulis C, Lycourghiotis A. Effect of temperature on the point of zero charge and surface charge of TiO_2. *J Chem Soc Faraday Trans.* 1990;86:3437-3440.

Manuscript received Jan. 13, 2004, and revision received July 20, 2004.